Direct-comb molecular spectroscopy with accurate, resolved comb teeth over 43 THz

A. M. Zolot,[1,*] F. R. Giorgetta,[1] E. Baumann,[1] J. W. Nicholson,[2] W. C. Swann,[1] I. Coddington,[1] and N. R. Newbury[1]

[1]*National Institute of Standards and Technology, 325 Broadway, Boulder, Colorado 80305, USA*

[2]*OFS Laboratories, 19 Schoolhouse Road, Suite 105, Somerset, New Jersey 08873, USA*

**Corresponding author: Alex.Zolot@nist.gov*

Received November 3, 2011; revised December 23, 2011; accepted December 24, 2011; posted January 4, 2012 (Doc. ID 157490); published February 10, 2012

We demonstrate a dual-comb spectrometer using stabilized frequency combs spanning 177 to 220 THz (1360 to 1690 nm) in the near infrared. Comb-tooth-resolved measurements of amplitude and phase generate over 4×10^5 individually resolved spectral elements at 100 MHz point spacing and kilohertz-level resolution and accuracy. The signal-to-noise ratio is 100 to 3000 per comb tooth. Doppler-broadened phase and amplitude spectra of CO_2, CH_4, C_2H_2, and H_2O in a 30 m multipass cell agree with established spectral parameters, achieving high-resolution measurements with optical bandwidth generally associated with blackbody sources.

OCIS codes: 300.6300, 320.7090.

The utility of frequency combs as "frequency rulers" is well established, and recent work has extended their use to direct spectroscopy of molecules [1–8]. Such effort has been motivated by many unique properties of frequency combs, including broad bandwidth, discrete spectral components (i.e., comb teeth), high spectral coherence, facile mixing to other spectral regions, and the potential for highly accurate frequency measurements [1]. For example, a "metrology" frequency comb covers an octave of bandwidth, comprising a million or more individual comb teeth, each with a well-defined frequency. However, several factors complicate the realization of all these potential benefits in a single spectrometer: spectral intensity variation stresses detection dynamic range, low comb tooth power limits the signal-to-noise ratio (SNR), and the individual detection of a million comb teeth requires an overwhelming number of detection channels. As a result, compromises are usually made. Many systems combine multiple teeth onto one detection channel, which improves SNR and reduces the sampling burden, but also reduces resolution and irrevocably forfeits the frequency-ruler nature of the comb.

Here, we demonstrate tooth-resolved direct-comb spectroscopy with at least 3× greater spectral bandwidth than previous dual-comb demonstrations. Broad supercontinuum (SC) sources have also been used in traditional spectrometers, but at lower resolution [1,9,10]. We use two fiber laser based frequency combs broadened to a 40 THz SC. The high mutual coherence of the combs allows measurement of the phase and amplitude response at each comb tooth as well as coherent averaging for high SNR. Moreover, each comb tooth has a known absolute frequency, linked to an H-maser, and ~kHz absolute linewidth, yielding spectral measurements with a similarly accurate and resolved frequency base.

A dual-comb spectrometer works by interfering two optical frequency combs with different repetition rates (and thus comb tooth spacing) of f_r and $f_r + \Delta f_r$ to directly map the comb teeth onto an rf multiheterodyne comb with tooth spacing Δf_r. Dual-comb spectrometers have been demonstrated in the terahertz, mid-infrared and near infrared with varying implementations [2–8]. Some demonstrations have focused on the high acquisition speed possible at relatively low resolutions, averaging over many teeth [2,6]. Here, we follow [3,4] and focus on long integration periods with highly coherent system so that individual comb teeth are fully resolved.

As outlined in Fig. 1, the spectrometer is based on two amplified and broadened mode-locked erbium fiber ring lasers pulsing at $f_r \sim 100$ MHz and $\lambda = 1560$ nm [3–5]. Each ring laser generates an optical frequency comb with ~2.5 THz optical bandwidth and 5–10 mW power. The

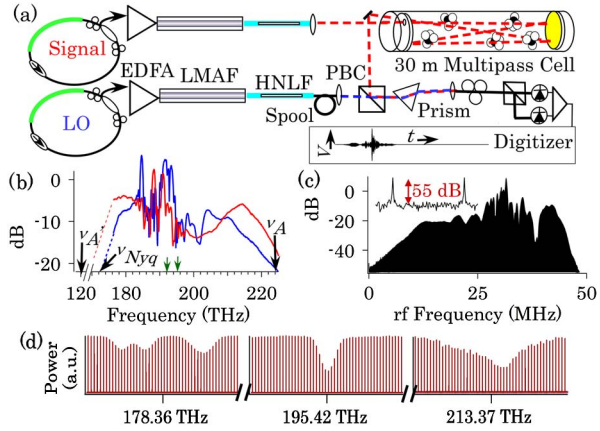

Fig. 1. (Color online) (a) Experimental schematic. Free-space optical paths indicated by dashes. EDFA, erbium-doped fiber amplifier; PBC, polarization beam cube. The digitizer signal, i.e., interferogram, is for a 40 THz SC recorded in $1/\Delta f_r = 10$ ms. (b) Sample signal (red) and LO (blue) comb optical spectra. Green arrows mark the two reference-cavity-stabilized cw laser frequencies. (c) Magnitude of the rf multiheterodyne spectrum from dual-comb interference, comprised of well-resolved 1 Hz teeth separated by 95 Hz, as shown in the top 140 Hz wide trace. The rf spectrum maps to the optical via $0 \rightarrow \nu_A, f_{rep}/2 \rightarrow \nu_{Nyq}$. (d) Corresponding comb-tooth-resolved optical spectra in 5 GHz windows across the $2\nu_3$ P5 lines in CH_4, $\nu_1 + \nu_3$ P15 line in C_2H_2, and $\nu_1 + \nu_3$ P6 line in H_2O. Structured H_2O line shapes result from differential absorption in the low-pressure multipass cell and in the high-pressure interferometer free-space path. Typical comb tooth extinction ratios are 500 : 1.

output is amplified to ~300 mW, the pulses compressed to 150 fs in 50 cm of anomalous-dispersion, large-mode-area fiber (LMAF) [11], and the spectrum broadened to 1360–1690 nm in highly nonlinear fiber (HNLF) with low normal dispersion of $<|-1.5$ ps/[km · nm]| [12]. The SCs from the nominally identical sources differ due to strong sensitivity to polarization and pulse shape. The choice of normal dispersion HNLF greatly reduces the relative intensity noise (RIN) of the SC compared to [10].

After broadening, the local oscillator (LO) comb pulses are stretched in 700 m of single-mode fiber to avoid saturation of the rf amplifiers [7]. The signal comb passes through a 30 m multipass gas cell. The signal and LO combs are combined, coupled into fiber, detected on a balanced photodiode, and digitized synchronously with the LO pulses at f_r. A prism prior to the fiber coupler produces a tunable 8 THz FWHM optical bandpass filter. It can be removed to detect the entire SC bandwidth. Attenuators limit the total power to ~60 μW for the filtered data to avoid photodetector nonlinearity [4], and to ~800 μW for the unfiltered data to maximize SNR.

If the relative linewidth of the comb teeth is less than Δf_r, the heterodyne signal between the combs generates resolved rf comb teeth with a one-to-one mapping back to the source comb teeth. We attain a relative comb linewidth of 1 Hz (and thus unambiguous mapping with comb tooth resolution) by phase locking each comb to a pair of reference-cavity-stabilized cw lasers. To avoid aliasing, the offset of the phase locks are set so that the signal and LO comb teeth are equal at two anchor points, ν_A and ν'_A, selected such that the SC falls between ν_A and the effective Nyquist frequency $\nu_{\mathrm{Nyq}} = (\nu_A + \nu'_A)/2$ [Fig. 1(b) and 1(c)]. The absolute frequencies of the cw lasers are measured with respect to the NIST H-maser with a separate metrology comb. Reference cavity drift of ~1–5 Hz/s between such measurements limits absolute frequency knowledge, and the resolution of each point, to below 10 kHz.

In one acquisition mode, a 1–5 s data stream is Fourier transformed to yield an rf spectrum with fully resolved comb teeth [Fig. 1(c) inset] and a correspondingly comb-tooth-resolved optical spectrum [Fig. 1(d)]. However, the acquisition duration in this mode is limited and does not support high SNR. Therefore, in a second acquisition mode, the data are also digitized continuously, but the successive, coherent interferograms are sequentially averaged point-by-point with a field-programmable gate array in real time before saving. (For the full SC, the interferograms are $2^{20} \sim 10^6$ points long.) This process reduces memory burden and enables data to be taken without dead time or loss of resolution, such that each point generated by the Fourier transform exactly corresponds to an individual signal comb tooth [3–5]. Real-time averaging only works for periods below the ~1 s mutual coherence time of the combs, beyond which the interferograms are no longer in phase. Therefore, the averaged data are saved at 0.5 s intervals, and a linear phase correction is applied before they are summed [4,5]. The resulting time-domain SNR of the interferogram then continues to increase with the square root of acquisition period [Fig. 2(a)].

The Fourier transformed averaged interferogram, scaled to the optical, yields the complex spectrum, $S(\nu) = S_0(\nu)\exp[-\alpha(\nu)L/2 - i\varphi(\nu)] + n(\nu)$, where $S_0(\nu)$ is the product of the LO and signal comb electric fields, αL and φ are the absorbance and phase shift from the gas sample's complex response, and $n(\nu)$ is the cumulative noise from detector noise, shot noise, SC RIN, and time variations in both the SC and unintentional etalons in the beam paths. This noise will have a component in-phase with $S(\nu)$, with standard deviation σ_I, and an out-of-phase component with standard deviation σ_Q. Here, we evaluate σ_I and σ_Q over a 5 GHz window, selected to be much wider than the Doppler-broadened linewidths of ~600 MHz for absorbance or ~1 GHz for phase.

We first remove unintentional etalons in the beam path, which can lead to 0.15% spectral ripple, by calculating the normalized quantity $-\ln[S_0(\nu)/S_{0R}(\nu)]$, where $S_{0R}(\nu)$ is a smoothed reference spectrum taken with an evacuated cell. The normalized response does not have a perfectly flat baseline due to the slowly changing SC, and a third-order polynomial fit is used to remove residual baseline wander. (SC variations could be removed experimentally over windows broader than 5 GHz through interleaved reference monitoring [3], at the cost of comb tooth resolution.) The standard deviation of the baseline-flattened spectrum over regions with no detectable absorption lines yields the noise, shown in Fig. 2(b) for the prism-filtered data at 180 THz. For all datasets, we find $\sigma_I = \sigma_Q = \sigma$ and, moreover, the noise is constant over frequency except for a very few isolated anomalous noise spikes. [One such spike occurs near 178.5 THz and is omitted in Fig. 2(b).] For prism-filtered data at 195 THz, the noise is entirely explained by the roughly equal contributions of detector and shot noise. For the prism-filtered data at 180 THz [see Fig. 2(b)], the noise is double this value either due to time-varying etalon effects or unsuppressed SC RIN (–137 dBc/Hz would account for the additional noise). At the higher 800 μW powers used for the full SC, there is some noise suppression due to detector saturation, but at the cost of distorted line shapes.

We define spectral SNR as $\mathrm{SNR}(\nu) = |S(\nu)|/\sigma(\nu)$, with a corresponding noise on the phase $\varphi(\nu)$ of $\mathrm{SNR}^{-1}(\nu)$ and on the absorbance $\alpha(\nu)L$ of $2\mathrm{SNR}^{-1}(\nu)$. Figure 3 shows the measured $\mathrm{SNR}(\nu)$ across the full SC over 122 min for a mixture of methane (CH_4), acetylene (C_2H_2), carbon dioxide (CO_2), and water (H_2O) at pressures of 58, 4.1, 470, and 1.9 Pa, respectively. Also shown is $\mathrm{SNR}(\nu)$ for three prism-filtered spectra of 23 Pa of CH_4 in 44 min, 2.3 Pa of C_2H_2 in 66 min, and 1.6 Pa of H_2O in 33 min.

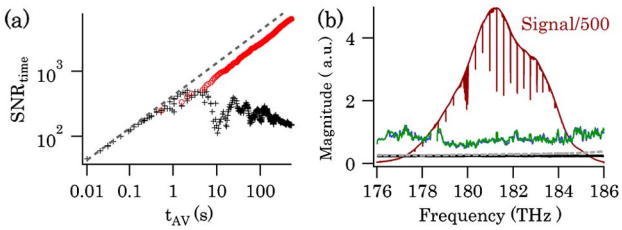

Fig. 2. (Color online) (a) Time-domain SNR without (black) and with (red) linear phase correction as a function of acquisition period, t_{AV}. The SNR increases as $t_{AV}^{1/2}$ (dashed gray). (b) The measured spectral magnitude, $|S_0(\nu)|$, (red) and the corresponding in-phase noise, σ_I, (blue) and out-of-phase noise, σ_Q, (green) for prism-filtered data near 180 THz. The dips are methane absorption lines. Also shown are shot noise (black) and detector noise (gray dashes).

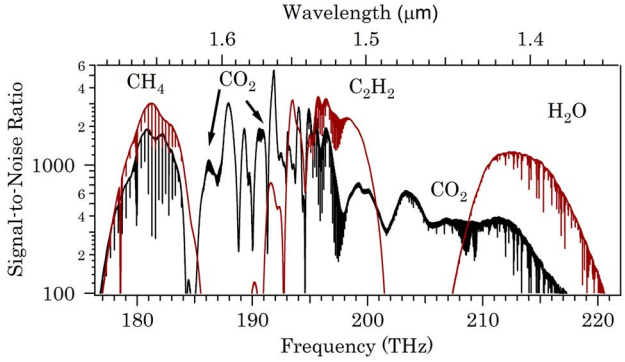

Fig. 3. (Color online) Spectral SNR measured across the full SC (black), and for filtered spectra (red). The full SC data spans 40 THz or 4×10^5 individual spectral elements with SNR > 100. For the filtered data, the broadband SNR exceeds 3000, yielding a phase noise of 1/SNR = 330 μrad and absorbance noise of 2/SNR = 6.6×10^{-4}. The full SC and prism-filtered data give normalized SNRs of 16 $s^{-1/2}$ and 53 $s^{-1/2}$ near 181 THz, respectively, including the time for the normalization spectrum acquisition.

Finally, Fig. 4(a) shows the measured absorbance and phase across the SC and Fig. 4(b) shows fits to several lines for the high-SNR prism-filtered data. The fitted intensities match existing Fourier transform spectroscopy (FTS) data [13] to within our 5% pressure uncertainty, and relative intensities match to 1%–2%. Line centers agree to within the ~10 MHz uncertainties of the FTS data. However, our absolute frequency accuracy is much better; a complete evaluation of systematics is ongoing, though related work in the mid-IR obtained uncertainty of 300 kHz, limited by photodetector nonlinearities [4].

Experimental sensitivity can be characterized as follows. A series of isolated Doppler-broadened lines have been least-squares fitted, providing an integrated absorbance uncertainty of ~0.2 MHz at SNRs of ~3000. Dividing by the Doppler width, the corresponding peak absorption sensitivity is 4×10^{-4}, corresponding to 10^{-7} absorbance per centimeter path length. The corresponding single-line column-density sensitivity is 6×10^{15} molecules/cm^2 and 3×10^{17} molecules/cm^2 for the CH_4 180 THz band and CO_2 190 THz band, respectively.

We have demonstrated a dual-comb spectrometer capable of fully resolving the phase and amplitude response on a tooth-by-tooth basis over 43 THz of spectral bandwidth. The spectrometer can probe multiple species of interest simultaneously, or select a subset of the bandwidth for increased SNR. This work demonstrates that the dual-comb technique can acquire high resolution and accurate laser-based spectra with many tens of terahertz bandwidth.

We thank Masaaki Hirano of Sumitomo Electric Industries for the donation of the HNLF fiber, and Frank Quinlan and Young-Jin Kim for valuable comments. F. R. Giorgetta received support from the Swiss National Science Foundation (SNSF) under grant PBNEP2-127797.

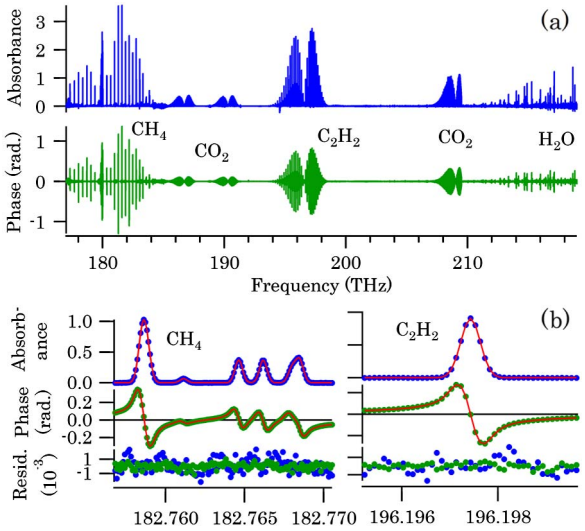

Fig. 4. (Color online) (a) Measured absorbance (blue) and phase (green) spectra. (b) Expanded view of the prism-filtered CH_4 $2\nu_3$ R8 region and C_2H_2 $\nu_1 + \nu_3$ P9 line. The symbols are the 100 MHz spaced measurements at the frequencies of comb teeth. Solid lines are fits to Doppler-limited line shapes, Gaussian function for the absorbance, and Dawson function for the phase [4].

References

1. F. Adler, M. J. Thorpe, K. C. Cossel, and J. Ye, Annu. Rev. Anal. Chem. **3**, 175 (2010).
2. A. Schliesser, M. Brehm, F. Keilmann, and D. van der Weide, Opt. Express **13**, 9029 (2005).
3. I. Coddington, W. C. Swann, and N. R. Newbury, Phys. Rev. Lett. **100**, 013902 (2008).
4. E. Baumann, F. R. Giorgetta, W. C. Swann, A. M. Zolot, I. Coddington, and N. R. Newbury, Phys. Rev. A **84**, 062513 (2011).
5. I. Coddington, W. C. Swann, and N. R. Newbury, Phys. Rev. A **82**, 043817 (2010).
6. B. Bernhardt, A. Ozawa, P. Jacquet, M. Jacquey, Y. Kobayashi, T. Udem, R. Holzwarth, G. Guelachvili, T. W. Hänsch, and N. Picqué, Nat. Photon. **4**, 55 (2010).
7. J. D. Deschenes, P. Giaccari, and J. Genest, Opt. Express **18**, 23358 (2010).
8. T. Yasui, M. Nose, A. Ihara, K. Kawamoto, S. Yokoyama, H. Inaba, K. Minoshima, and T. Araki, Opt. Lett. **35**, 1689 (2010).
9. J. Mandon, E. Sorokin, I. T. Sorokina, G. Guelachvili, and N. Picqué, Opt. Lett. **33**, 285 (2008).
10. C. A. Michaels, T. Masiello, and P. M. Chu, Appl. Spectrosc. **63**, 538 (2009).
11. J. W. Nicholson, A. D. Yablon, M. F. Yan, P. Wisk, R. Bise, D. J. Trevor, J. Alonzo, T. Stockert, J. Fleming, E. Monberg, F. Dimarcello, and J. Fini, Opt. Lett. **33**, 2038 (2008).
12. M. Hirano, T. Nakanishi, T. Okuno, and M. Onishi, IEEE J. Sel. Top. Quantum Electron. **15**, 103 (2009).
13. A. V. Nikitin, O. M. Lyulin, S. N. Mikhailenko, V. I. Perevalov, N. N. Filippov, I. M. Grigoriev, I. Morino, T. Yokota, R. Kumazawa, and T. Watanabe, J. Quant. Spectrosc. Radiat. Transfer **111**, 2211 (2010).